Applied Microbiology and Biotechnology (2024) 108:462
https://doi.org/10.1007/s00253-024-13282-4

BIOTECHNOLOGICAL PRODUCTS AND PROCESS ENGINEERING

# Exploration of diverse secondary metabolites from *Penicillium brasilianum* by co-culturing with *Armillaria mellea*

**Xiaoting Rong[1] · Lihua Zhang[2] · Wenni He[1] · Zhe Guo[1] · Hui Lv[1] · Jinglin Bai[1] · Liyan Yu[1] · Lixin Zhang[3] · Tao Zhang[1]**

Received: 21 April 2024 / Revised: 7 August 2024 / Accepted: 14 August 2024 / Published online: 12 September 2024


## Abstract

Bioinformatic analysis revealed that the genomes of ubiquitous *Penicillium* spp. might carry dozens of biosynthetic gene clusters (BGCs), yet many clusters have remained uncharacterized. In this study, a detailed investigation of co-culture fermentation including the basidiomycete *Armillaria mellea* CPCC 400891 and the *P. brasilianum* CGMCC 3.4402 enabled the isolation of five new compounds including two bisabolene-type sesquiterpenes (arpenibisabolanes A and B), two carotane-type sesquiterpenes (arpenicarotanes A and B), and one polyketide (arpenichorismite A) along with seven known compounds. The assignments of their structures were deduced by the extensive analyses of detailed spectroscopic data, electronic circular dichroism spectra, together with delimitation of the biogenesis. Most new compounds were not detected in monocultures under the same fermentation conditions. Arpenibisabolane A represents the first example of a 6/5-fused bicyclic bisabolene. The bioassay of these five new compounds exhibited no cytotoxic activities in vitro against three human cancer cell lines (A549, MCF-7, and HepG2). Moreover, sequence alignments and bioinformatic analysis to other metabolic pathways, two BGCs including *Pb-bis* and *Pb-car*, responsible for generating sesquiterpenoids from co-culture were identified, respectively. Furthermore, based on the chemical structures and deduced gene functions of the two clusters, a hypothetic metabolic pathway for biosynthesizing induced sesquiterpenoids was proposed. These results demonstrated that the co-culture approach would facilitate bioprospecting for new metabolites even from the well-studied microbes. Our findings would provide opportunities for further understanding of the biosynthesis of intriguing sesquiterpenoids via metabolic engineering strategies.

## Key points

- *Penicillium and Armillaria co-culture facilitates the production of diverse secondary metabolites*
- *Arpenibisabolane A represents the first example of 6/5-fused bicyclic bisabolenes*
- *A hypothetic metabolic pathway for biosynthesizing induced sesquiterpenoids was proposed*

**Keywords** Co-culture · *Penicillium brasilianum* · *Armillaria mellea* · Secondary metabolites · Sesquiterpenes

Xiaoting Rong and Lihua Zhang contributed equally to this work.

✉ Liyan Yu
yly@cpcc.ac.cn

✉ Lixin Zhang
lxzhang@ecust.edu.cn

✉ Tao Zhang
tzhang_0218@163.com

[1] Institute of Medicinal Biotechnology, Chinese Academy of Medical Sciences & Peking Union Medical College, Beijing 100050, China

[2] National Key Laboratory of Chinese Medicine Modernization, State Key Laboratory of Component-Based Chinese Medicine, Institute of Traditional Chinese Medicine, Tianjin University of Traditional Chinese Medicine, Tianjin 301617, China

[3] State Key Laboratory of Bioreactor Engineering, East China University of Science & Technology, Shanghai 200237, China

## Introduction

Filamentous fungi have been demonstrated to be an important source of agrochemicals, pharmaceutical drugs, and other chemical agents (Bills and Gloer 2016; Keller 2019; Zhang et al. 2023b, 2013). However, it is becoming increasingly difficult to screen novel lead compounds by conventional chemical-only strategies for high frequency of repeated discovery of known metabolites (Malit et al. 2022). The fact that the metabolic potential has not yet been exploited is due to the observation that most gene clusters are transcriptionally silent under normal laboratory culture conditions. Furthermore, genome sequencing has revolutionized secondary metabolites (SMs) mining efforts, manifesting that the capacity of filamentous fungi to produce compounds was far more than we anticipated previously (Keller 2019; Medema et al. 2021). To circumvent these limitations, several strategies have been conducted to trigger cryptic biosynthetic pathways, exemplified as "one strain many compounds (OSMAC)" approach (Bode et al. 2002; Pan et al. 2019; Zhang et al. 2022a), metabolic engineering of targeted pathways (Zhang et al. 2022b, 2018), epigenetic modification (Cichewicz 2010; Mao et al. 2015; Zheng et al. 2022), heterologous expression of gene clusters using different host (Lyu et al. 2021; Oikawa 2020; Zhang et al. 2023a), and co-culture (Bertrand et al. 2014; Wang et al. 2022; Zhuang and Zhang 2021). Previous studies have demonstrated that co-culture methodology is effective in facilitating the discovery of new SMs with fascinating structures (Knowles et al. 2022; Park et al. 2017). Thus, the genome-guided co-culturing approach renders the isolation of bioactive molecules efficient and promising.

Cell–cell interactions of different microorganisms could simulate the competition of natural ecosystems (Ghoul and Mitri 2016; Weiland-Brauer 2021), and the cryptic metabolic pathways are transcriptionally triggered by interspecies crosstalk or environmental stimuli (Zhang et al. 2022a). The presence of another strain population might stimulate strain behavior or culturing success (Goers et al. 2014). Also, the chemical inducer released from other microbes might cause defense responses, which include yielding diverse arrays of SMs, secretion of extracellular enzymes, the synergistic act of biotransformation, or signaling pathways activation (Bouws et al. 2008; Elhamouly et al. 2022). Co-culture systems are highly relevant and could find myriad applications in mining metabolites based on the natural interactions between cell populations. Recently, the microbial co-culture-based SMs mining approach has attracted increasing interest, as exemplified by bacterial-bacterial (Sugiyama et al. 2019), fungal-bacterial (Park et al. 2017), and fungal-fungal co-cultivation systems (Wang et al. 2018). These studies highlighted the capability of co-culture to effectively trigger the generation of metabolites (Kim et al. 2021). Thus, the different co-culture systems have increased productivity over monocultures and hold greater potential for mining novel compounds.

*Penicillium* is a diverse genus occurring worldwide composed of 354 accepted species (Visagie et al. 2014), and a large number of SMs exhibiting potent bioactivities and intriguing structural features are reported from *Penicillium* genus, such as polyketides, alkaloids, peptides, terpenoids, and hybrids (Brase et al. 2009; Kozlovsky et al. 2020). *P. brasilianum* could produce compounds including griseofulvin, verruculogen, brasiliamides, and meroterpenoids, and has been an interesting fungus to many researchers in the continuous screening for new compounds (Bazioli et al. 2017). Metabolomic profiling of *Armillaria* on rice medium was previously performed indicating that only a small subset of metabolites could be produced (Zhang et al. 2022a). Additionally, genomic analysis further revealed a rich repertoire of genes in *Armillaria* encoding cytochrome P450s and plant cell wall–degrading enzymes (PCWDEs) genome (Zhang et al. 2022a, 2023a). Therefore, a scaled-up fermentation of the co-culture system composed of *P. brasilianum* and the *A. mellea* was performed. In the present study, systematic chemical investigation enabled the isolation of five new compounds, including two bisabolene-type sesquiterpenes, named arpenibisabolanes A and B (**1**–**2**), two carotane-type sesquiterpenes, named arpenicarotanes A and B (**3**–**4**), and one polyketide, arpenichorismite (**5**), together with seven known compounds. Notably, some of the new compounds (**1**–**5**) were not produced by either of the two fungi when cultivated alone under the same fermentations, and arpenibisabolanes A (**1**) represents the first example of a 6/5-fused bicyclic bisabolene. Herein, we described the isolation and structural elucidation of these metabolites. The BGCs and hypothetical metabolic pathways for biosynthesizing induced sesquiterpenoids were also investigated.

## Materials and methods

### Fungal strains and culture conditions

The fungi *P. brasilianum* CGMCC 3.4402 (NBRC 6234) and *A. mellea* CPCC 400891 (DSM 3731) used in this study were deposited in the China Pharmaceutical Culture Collection Center (CPCC). The fungi were routinely cultivated on potato dextrose medium (PDA) and preserved in 15% glycerol at − 80 °C. The growth temperature of the strains is 28 °C. OSMAC-based evaluation of strain NBRC 6234 producing secondary metabolites was conducted using eight

different culture media as performed previously: PDB broth, YMEG broth, MEP broth, F1 broth, F2 broth, CY broth, and rice medium (20 g rice/20 mL of deionized water in 250-mL Erlenmeyer flask) (Zhang et al. 2022a). The fermentation cultures include a two-stage process; the fungus *P. brasilianum* was cultivated on PDA media at 28 °C for 7 days and served as seed culture. The spores were harvested and inoculated equally into the fermentation medium (100 mL respective broth in 500-mL Erlenmeyer flasks) described above. The routine fermentation was cultivated for 10 days on a shaker (150 r/min) or incubated statically in rice medium for 25 days (Rong et al. 2023a, 2023b).

## Sequencing and bioinformatic tools

Genomic DNA (gDNA) from *Penicillium* was extracted from mycelia cultivated in PDB broth using E.Z.N.A.® Fungal DNA Mini Kit (Omega, Norcross, GA, USA) according to the manufacturer's instruction. Genome sequencing was conducted at Shanghai Majorbio Bio-pharm Technology Co. Ltd. (Shanghai, China) using the Illumina Hiseq 2000 platform. The contigs that were assembled and annotated by SOAPdenovo 1.05 were formatted to the UniProt database for BLAST alignment (Bateman et al. 2023; Luo et al. 2012). The AntiSMASH software was used for analysis of secondary metabolites biosynthetic gene clusters (BGCs) (Blin et al. 2019). Gene annotations of the coding sequences were deduced and verified manually based on the homologues in the NCBI database.

## Co-culturing approach and large-scale fermentation

For the fungus *A. mellea*, the cultivation was performed in MEP broth based on the details as previously reported (200 mL each in 500-mL Erlenmeyer flasks × 5) for 10 days (Zhang et al. 2022a, 2023a). For the *Penicillium* strain CGMCC 3.4402, it was cultivated in PDB broth (200 mL each in 500-mL Erlenmeyer flasks × 3) for 7 s days. The large-scale co-culture fermentation (6 kg rice) was carried out in Erlenmeyer flasks (100 g rice/100 mL of deionized water in 500-mL Erlenmeyer flask). The fungal strains were transferred into rice media simultaneously, in which the inoculants of *Penicillium* and *Armillaria* were 5 mL, respectively. The fermentations were cultured at 28 °C under static conditions for 30 days (Zhang et al. 2022b).

## Chemicals and chemical analysis

Circular dichroism spectra were recorded using a Jasco J-815 spectropolarimeter (Jasco, Tokyo, Japan). High-performance liquid chromatography (HPLC) analyses were carried out on an Agilent 1290 instrument with a YMC-Pack ODS-AQ column (4.6 × 250 mm, 5 μm). TLC was conducted on silica gel GF254 plates from Qingdao Marine Chemical, China. The medium-pressure liquid chromatography was carried out on Combi Flash Rf 200 (Teledyne Isco, Lincoln NE, USA) using a SEPAF FLASH® Flash silica gel column (40–63 μm, 60 Å, 330 g, Santai Technologies, China). The semi-preparative HPLC separations were performed on SSI series 1500 (Cometro Technology Ltd, NJ, USA) equipped with a DAD detector using a YMC-Pack ODS-AQ column (10.0 mm × 250 mm, 5 μm). High-resolution mass spectrometric data was obtained using a Thermo LTQ Orbitrap XL Mass Spectrometer installed with an electrospray ionization source (Thermo Fisher Scientific, CA, USA). Nuclear magnetic resonance (NMR) data were acquired on a Bruker AVIII-600 spectrometer using TMS as internal standard (150 MHz for $^{13}C$ NMR and 600 MHz for $^{1}H$ NMR, Bruker Corporation, Germany), which were measured in $CDCl_3$ or $CD_3OD$.

## Extraction and isolation of secondary metabolites

After the fermentation period, the cultures of different fermentation media were centrifuged to harvest the mycelia from broth, respectively (5500 r/min, 15 min). The supernatant and respective fungal material were extracted twice with ethyl acetate (EtOAc) separately and successively combined to afford one sample (Zhang et al. 2022a). The culture of rice medium was directly extracted using EtOAc twice. All seven solutions were collected and concentrated in vacuo to dryness. Each crude extract was redissolved in MeOH and analyzed following the same methodology described previously (Rong et al. 2023a, 2023b).

The co-culture materials were extracted repeatedly with MeOH (3 × 25 L), and the successive MeOH extracts were combined and evaporated under vacuum yielding 300 mL of crude extracts. The materials were fractionated with *n*-hexane (3 × 200 mL) and EtOAc (4 × 500 mL), and the EtOAc solvent was evaporated to dryness under rotatory evaporation to yield the crude extract (ca. 22 g). The crude extract was subsequently separated on silica gel (200–300 mesh) column chromatography (12 cm × 40 cm). The column was eluted with a gradient consisting of $CHCl_2$/MeOH (v/v, 100:0 → 95:5 → 90:10 → 85:15 → 80:20 → 75:25 → 70:30 → 65:35 → 60:40 → 55:45 → 50:50 → 45:55 → 40:60 → 0:100), to obtain 10 fractions (Fr.1–Fr.10). Fr.6 was further separated by ODS column, using a stepped gradient elution of $CH_3CN$-$H_2O$ (20:80 to 100:0) to yield 14 subfractions (Fr.6–1 to Fr.6–14). Fraction Fr.6–2 was purified by pHPLC eluted with $CH_3CN$-$H_2O$ (0.01% TFA) (20:80) to afford compound **9** (6.8 mg, $t_R$ = 8.0 min). Purification of fraction Fr.6–9 was conducted by semi-preparative HPLC, eluting

with $CH_3CN$-$H_2O$ (0.01% TFA) (25:75) to afford compounds **3** (4.6mg, $t_R$ = 25.8 min) and **7** (3.5 mg, $t_R$ = 26.8 min). Fraction Fr.6–3 was separated by semi-preparative HPLC with $CH_3CN$-$H_2O$ (0.01% TFA) (10:90) to yield compounds **12** (3.5 mg, $t_R$ = 11.0 min), **10** (3.5 mg, $t_R$ = 18.0 min), and **11** (4.8 mg, $t_R$ = 20.0 min). Fraction Fr.6–5 was purified by pHPLC eluted with $CH_3CN$-$H_2O$ (0.01% TFA) (40:60) to obtain compound **1** (4.5 mg, $t_R$ = 13.0 min). Purification of fraction Fr.6–5 was conducted by semi-preparative HPLC, eluting with $CH_3CN$-$H_2O$ (0.01% TFA) (40:60) to afford compound **2** (4.5 mg, $t_R$ = 13.0 min). Purification of fraction Fr.6–6 was performed by pHPLC, using $CH_3CN$-$H_2O$ (0.01% TFA) (40:60) to obtain compound **4** (7.2 mg, $t_R$ = 7.0 min) and compound **6** (5.7 mg, $t_R$ = 5.4 min). Fraction Fr.5 was eluted with a gradient using a silica gel column $CH_3CN$-$H_2O$ (20:80 to 100:0) to yield 13 subfractions (Fr.5–1 to Fr.5–13). Fraction Fr.5–2 was purified by semi-preparative HPLC with $CH_3CN$-$H_2O$ (0.01% TFA) (15:85) to obtain compound **8** (14.4 mg, $t_R$ = 25.0 min). Fraction Fr.5–4 was purified by pHPLC eluted with $CH_3CN$-$H_2O$ (0.01% TFA) (25:75) to acquire compound **5** (10.9 mg, $t_R$ = 15.0 min).

## Electronic circular dichroism (ECD) calculation of 1 – 4

Stochastic conformational searches were firstly conducted under MMFF94 force field for **1 – 4** and gave their conformers. Their conformers were optimized at the B3LYP/6-31G(d) basis set level in methanol, and the frequencies were calculated by further time-dependent density functional theory (TDDFT) method, indicating that these conformers were stable. Using the conformers at the B3LYP/6-31G(d) basis set level in methanol, their excitation states at the B3LYP/6-31G(d) basis set level were calculated, peak stretcher was 0.4 eV, and finally the calculation results were Boltzmann averaged to yield the depicted electronic circular dichroism (ECD) spectra of **1 – 4**. All calculations were performed by Gaussian 09 program package (Version C.01).

## Cytotoxic activity assays

Five new metabolites were tested for their cytotoxic activities as previously reported methods (Rong et al. 2023a, 2023b; Zhang et al. 2022a). Briefly, cells ($3 \times 10^4$ cells/mL) were inoculated in the wells of a 96-well plate at 100 µL/well. After 24 h of incubation at 37 °C and 5% $CO_2$, cells were cultivated to 90% confluence. Carcinogenic cell lines including A549, MCF-7, and HepG2 were treated with gradient concentrations of isolated compounds for 48 h (DMSO and cisplatin were used as negative and positive controls, respectively). The concentration gradient of cisplatin is 20, 10, 5, 2.5, 1.25, and 0.625 µM, respectively. The cytotoxicity was measured by the CCK-8 method (Zhang et al. 2022a). Measure the absorbance at 450 nm using a microplate reader (Bio-Rad, Fitchburg, WI, USA). The dilutions of the tested compounds were independently performed thrice. The half-maximal inhibitory concentration ($IC_{50}$) of compounds in three cell lines was calculated using GraphPad Prism 7. Purities of tested metabolites were > 95% detected by HPLC-ELSD.

## Gene *Pb_bisA* synthesis, yeast transformation, and GC–MS analysis

The candidate gene *Pb_bisA* was synthesized by GenScript and codon-optimized for expression in yeast. The oligonucleotide primers used for are listed in Table S1 (Supporting information). PCR reaction is performed using 2 × Phanta Max Master Mix (Vazyme) following the manufacturer's instructions. Yeast expression plasmid YET was used for construction of YET-*Pb_bisA* by in vivo homologous recombination strategy. Yeast transformation was conducted using a Frozen-EZ Yeast Transformation II Kit™ (Zymo Research). Yeast plasmid was prepared by a E.Z.N.A® Yeast Plasmid Miniprep Kit (Omega) and transformed into *E. coli* Trans-T1 (TransGen Biotech) for sequencing.

The fermentation and samples preparation for gas chromatography–mass spectrometry (GC–MS) analysis were performed as reported previously with minor modifications (Li et al. 2023b; Zhang et al. 2023a). The 5.0 mL cultures of yeast transformants were collected in the headspace (20 mL), followed by incubation at 55 °C for 20 min. The volatile components were harvested at 55 °C for 30 min by solid-phase micro-extraction (SPME) with a DVB/CAR/PDMS fiber. The samples were analyzed on an Agilent 7890B/5977A gas chromatography incorporated with an Agilent 7200 accurate-mass quadrupole time-of-flight (GC–MS-TOF) and a DB-WAX column (Agilent, 60 m × 0.25 mm ID, 0.25 µm film thickness). The system and the program were performed under the standard condition described previously (Li et al. 2023b; Zhang et al. 2023a). Full-scan mass spectra were recorded in the range of 100–300 m/z, and ionization was conducted by electron impact at 70 eV with an electrospray ionization source temperature adjusted at 230 °C.

# Results

## Constructing co-culture system to induce SMs production

To investigate the biosynthetic potential of *P. brasilianum*, we initially performed a whole genome sequencing of the fungus. The Illumina HiSeq 2500 sequencing of the strain

yielded a total of ~ 5148 million bases. Assembling of the unpaired reads generated 44 scaffolds, which consist of 34.12 million nonredundant bases. During the antiSMASH-guided bioinformatic analysis, forty BGCs were obtained and the potential biosynthetic compounds include polyketides (no. 12), nonribosomal peptides (no. 17), hybrids (no. 4), terpenes (no. 5), and beta lactones (no. 2). Subsequently, OSMAC approach was applied to evaluate the chemical diversity of the strain. However, the fungus did not biosynthesize many secondary metabolites in the rice medium, PDB broth, MEP broth, F1 broth, F2 broth, YMEG broth, or CY broth (Fig. S1, supporting information), which are commonly used for promoting chemodiveristy in filamentous ascomycetes (Ariantari et al. 2019; Zang et al. 2020). These results indicated that the OSMAC strategy could not broaden the structurally diverse pattern of SMs from the strain *P. brasilianum*.

The *A. mellea* exhibits a parasitic lifestyle and is widely distributed as devastating pathogens of herbaceous plants or broadleaf trees (Baumgartner et al. 2011; Fradj et al. 2020). Significantly, the *Armillaria* encode a large number of PCWDEs (Zhang et al. 2023a). Thus, this strain was believed to be capable of generating interaction with the *Penicillium* and served as an inducing strain of co-culture system. As a control, the culture of *Armillaria* strain alone resulted in a similar condition (Fig. 1, trace I; Fig. S2, supporting information). Markedly, chemical analysis of the strain *P. brasilianum* cultivated in rice medium resulted in a sparse metabolite profile, only a few dominating peaks were visible in the HPLC-ELSD chromatogram (Fig. 1, trace ii; Fig. S2, supporting information). However, the co-culture significantly stimulated the expression of BGCs and/or uncharacterized metabolic pathways (Fig. 1, trace iii; Figs. S2 and S3, supporting information). This demonstrates that the co-culture system is feasible, which could stimulate the production of new or uncharacterized SMs.

## Identification of induced metabolites from co-culture system

Compound **1** was obtained as colorless oil. The molecular formula $C_{15}H_{18}O_6$, with seven degrees of unsaturation, was determined by HR-ESI–MS at m/z 293.1020 $[M-H]^-$ (calcd for $C_{15}H_{17}O_6^-$ 293.1025). The 1D NMR (Table S2, supporting information) and HSQC data of **1** clearly displayed the presence of two carbonyls [$\delta_C$ 189.5 and 171.4], three double bonds [$\delta_C/\delta_H$ 148.3/7.69 (1H, s), 141.9/6.78 (1H, tq, $J=7.44$, 1.44 Hz); $\delta_C$ 141.7, 138.1, 130.2, 126.9], two methyls [$\delta_C/\delta_H$ 12.5/1.76 (3H, s), 18.2/1.30 (3H, s)], three methylenes [$\delta_C/\delta_H$ 29.5/2.48 (2H, m); 28.4/3.06 (1H, dd, $J=5.4$, 16.8 Hz), 2.58(1H, m); 22.8/2.62(2H, m)], and two oxygenated quaternary carbons [$\delta_C$ 79.3, 75.2] (Fig. 2). The key HMBC correlations (Fig. 3) of $H_3$-15/C-2, C-3, C-4; of H-2/C-3, C-6; of H-1/C-2, C-5, C-6, C-7; and H-14/C-5, C-6, C-7 led to the assignment of a bicyclic system consisted of a cyclohexanone ring fused with a furan ring through C-5 and C-6. Then, a C5 $\alpha$, $\beta$-unsaturated carboxylic acid side chain at C-7 could be inferred, supported by the molecular formula of **1** and the key HMBC correlations (Fig. 3) of H-13/C-10, C-11, C-12; of H-10/C-8, C-9, C-11, C-12; of H-9/C-7, C-8, C-11; and of H-8/C-1. Thus, the gross structure of **1** was established.

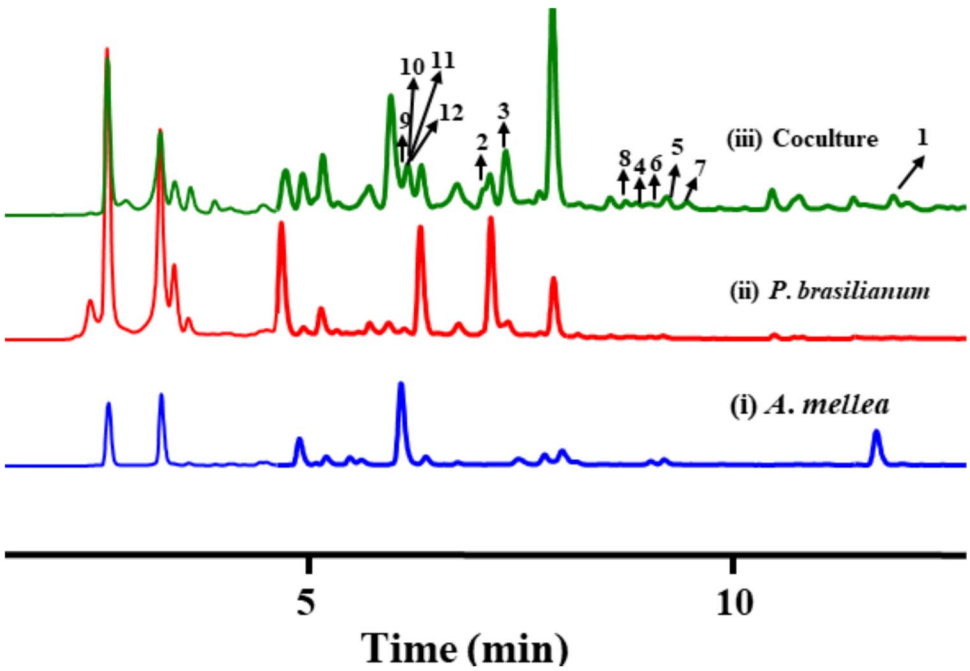


**Fig. 1** HPLC profiles of organic extracts obtained from the strain *P. brasilianum* by co-culture strategy. (i) *A. mella*; (ii) *P. brasilianum*; (iii) co-culture. The extracts were analyzed by measuring UV absorbance spectra at 230 nm on an Agilent 1290 Infinity system equipped with an Alltech ELSD 2000 detector

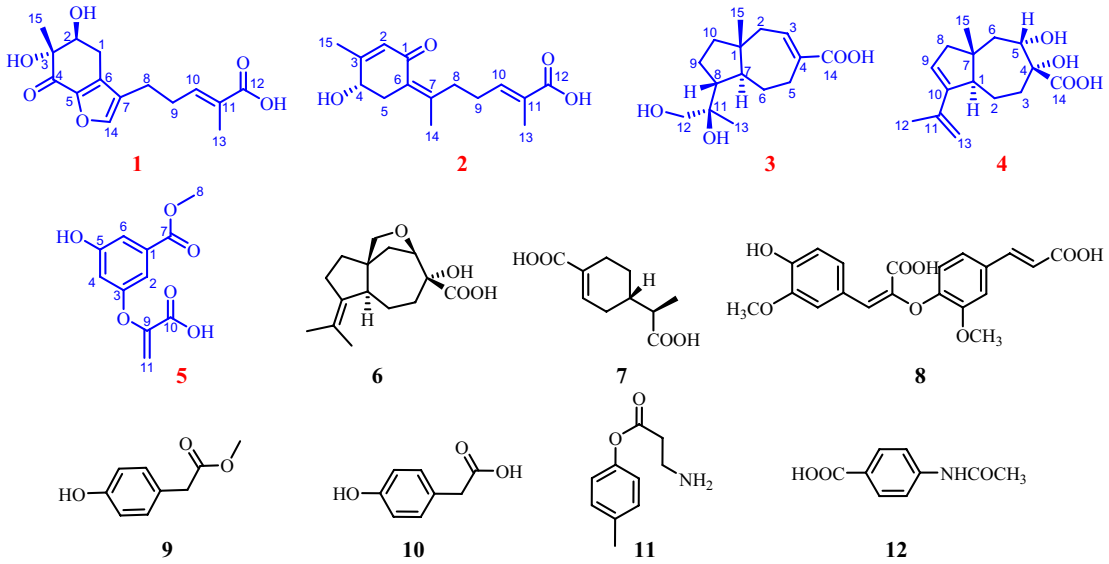


**Fig. 2** Structures of compounds **1**–**12** isolated in the study

Due to no available NOESY spectrogram, the relative configuration of C-2/C-3 could not be established. Further, the absolute configuration of **1** was assigned as 2*S*,3*R* by comparison of the experimental and calculated ECD spectra of four configurations (2*R*,3*R*-**1a**, 2*S*,3*S*-**1b**, 2*S*,3*R*-**1c**, 2*R*,3*S*-**1d**) (Fig. 4A and B). Accordingly, the absolute configuration of **1** was determined and characterized as arpenibisabolane A (Figs. S4–S11, supporting information).

The molecular formula of compound **2** was assigned as $C_{15}H_{20}O_4$ based on the HR-ESI–MS at m/z 263.1278 $[M\text{-}H]^-$ (calcd for $C_{15}H_{19}O_4^-$ 263.1283), corresponding to six degrees of unsaturation. Comparison of the 1D NMR data

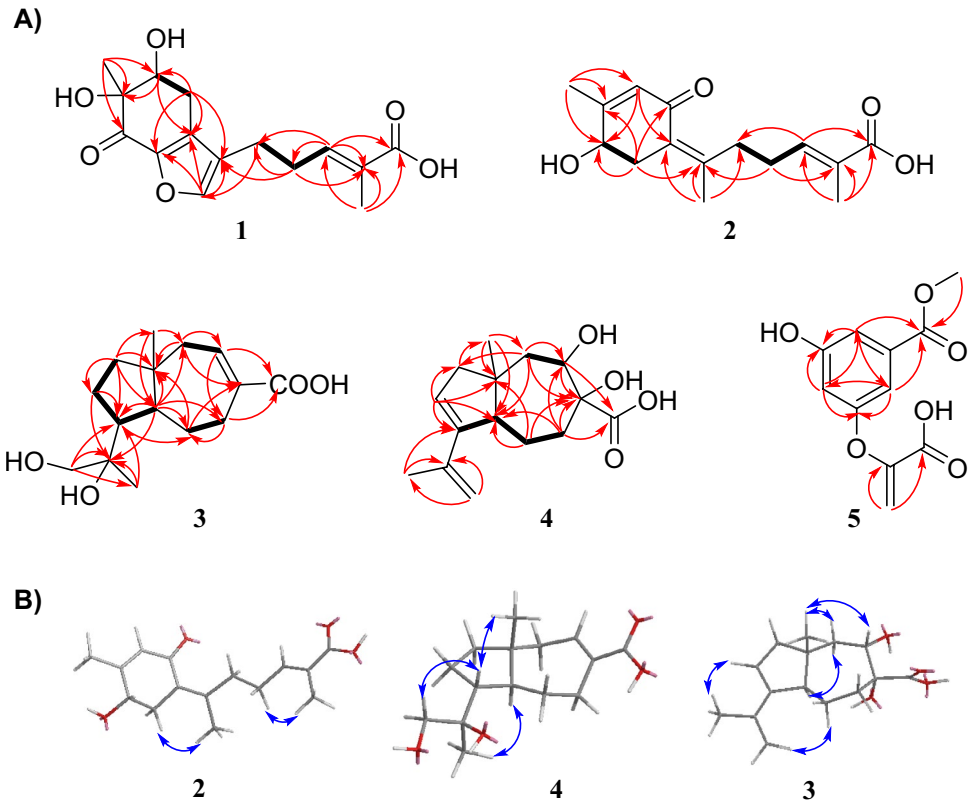


**Fig. 3** Key HMBC, COSY, and NOESY correlations of **1**–**5**. **A** Key HMBC and COSY correlations of **1**–**5**. **B** NOESY correlations of **2**–**4**

(Table S2, supporting information) of **2** with those of **1** indicated that **2** shared the identical $\alpha$, $\beta$-unsaturated carboxylic acid moiety. The remaining NMR data (Table S2, supporting information) corresponded to one carbonyl ($\delta_C$ 192.7), two double bonds [$\delta_C/\delta_H$ 129.5/5.84 (1H, m); $\delta_C$ 164.3, 129.3, 149.2], two methyls [$\delta_C/\delta_H$ 21.0/1.94 (3H, s), 20.2/2.02 (3H, s)], one methylene [$\delta_C/\delta_H$ 38. 0/3.0 (1H, m), 2.61 (1H, m)], and one oxygenated methine [$\delta_C/\delta_H$ 70.0/4.25 (1H, m)]. The key HMBC correlations (Fig. 2) of H-13/C-10, C-11, C-12; of H-10/C-8, C-12; of H-9/C-11; and of H-14/C-7, C-8 confirmed the presence of a $C_6$ $\alpha$, $\beta$-unsaturated carboxylic acid side chain (C-7–C-12). Then, one $\alpha$, $\beta$-unsaturated cyclohexanone moiety was deduced by the key HMBC correlations of $H_3$-15/C-2, C-3, C-4; of H-2/C-4, C-6; and $H_2$-5/C-1, C-3, C-4. Further, HMBC correlations of $H_3$-14/C-6 and $H_2$-5/C-7 led to the linkage of C-6/C-7 (Fig. 3). Thus, the gross structure of **2** was established (Fig. 2). The *E*-geometry of $\Delta^{10(11)}$ and *Z*-geometry of $\Delta^{6(7)}$ double bonds were assigned by the NOESY correlations (Fig. 3) of $H_3$-14/$H_2$-5 and $H_3$-13/$H_2$-9. The absolute configuration of **2** was determined by comparison of its experimental and calculated ECD data. The experimental ECD curve (Fig. 4C) of **2** agreed well with the calculated curve of 4*S*-**2a**, which assigned its absolute configuration as 4*S*. Thus, the structure of **2** was established and named arpenibisabolane B (Figs. S12–S20, supporting information).

Compound **3** has a molecular formula of $C_{15}H_{24}O_4$, which was deduced from its HR-ESI–MS data at m/z 291.1550

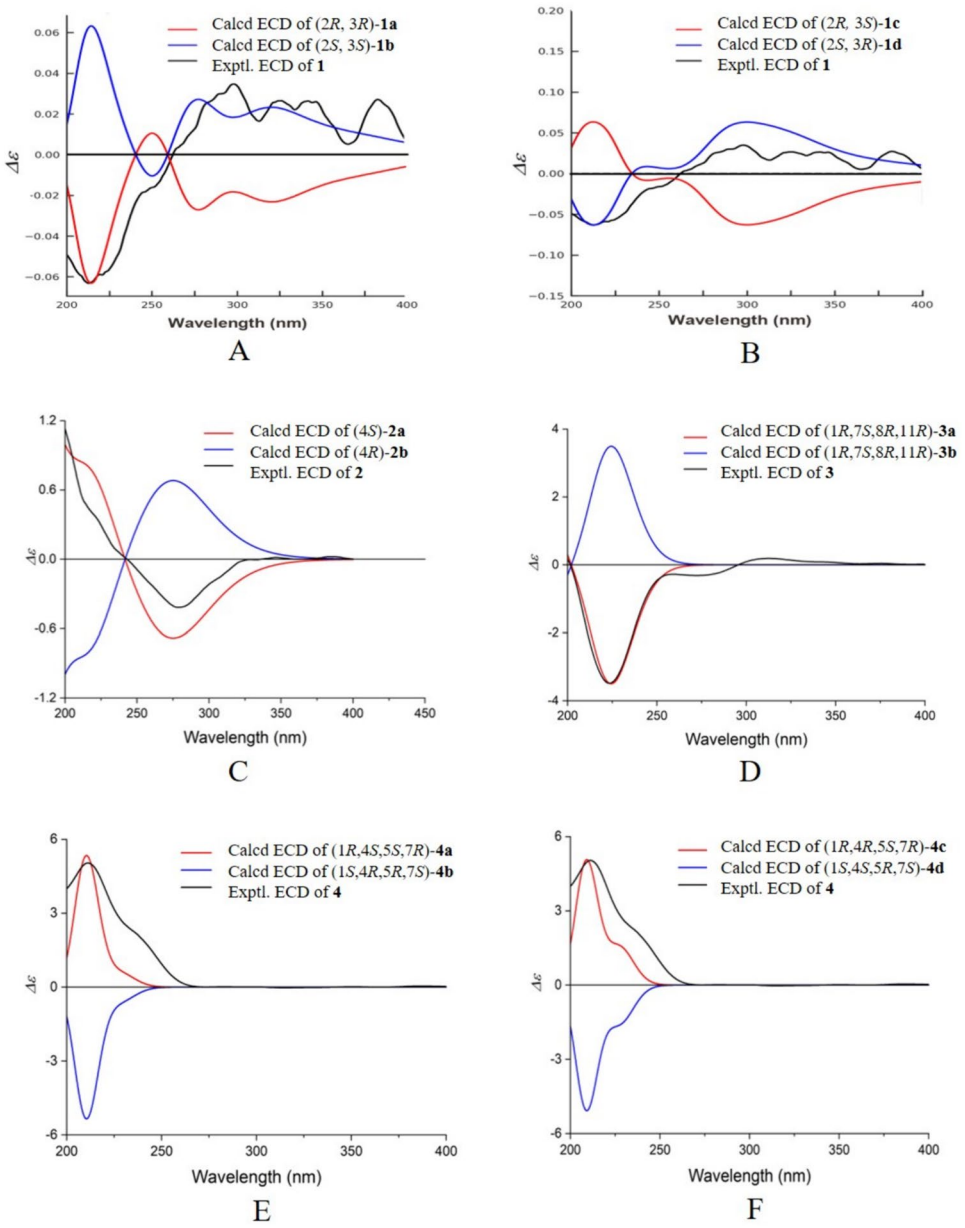


**Fig. 4** Calculated and experimental ECD spectra for compounds **1**–**4**. **A**, **B** Arpenibisabolane A (**1**). **C** Arpenibisabolane B (**2**). **D** Arpenicarotane A (**3**). **E**, **F** Arpenicarotane B (**4**) in MeOH

$[M+Na]^+$ (calcd for $C_{15}H_{24}O_4Na^+$ 291.1550), corresponding to four degrees of unsaturation. The $^1H$ NMR data (Table S3, supporting information) exhibited one olefinic proton at $\delta_H$ 7.07 (1H, m), two oxygenated methylenes at $\delta_H$ 3.40 (1H, d, $J=11.1$ Hz) and 3.36 (1H, d, $J=11.4$ Hz), and two methyls at $\delta_H$ 1.12 (3H, s) and 0.78 (3H, s). The $^{13}C$ NMR (Table S3, supporting information) and HSQC data revealed the existence of fifteen carbon signals, including one carbonyl, two $sp^2$ carbons, two methyls, five methylenes, three methines, and two quaternary carbons (Fig. 2). The key HMBC correlations (Fig. 3) of $H_3$-15/C-2, C-7; of $H_2$-2/C-1, C-3, C-4; of H-3/C-5, C-14; of $H_2$-5/C-6, C-14; of $H_2$-6/C-1, C-4; of H-7/C-1, C-2, C-5, C-6, C-8; of H-10/C-1, C-7, C-8, C-9, C-15; and of H-9/C-8 suggested the presence of a bicyclic system consisted of a cyclopentane fused with a cycloheptane with one methyl and one carboxyl respectively assigned at C-15 and C-4. Then, the key HMBC correlations (Fig. 3) of $H_3$-13/C-8, C-11; of $H_2$-12/C-8, C-11, C-13; of $H_2$-9/C-11; of H-7/C-11; of $H_3$-13/C-11, C-8; of $H_2$-12/C-8 and C-11, C-13; and of $H_2$-9/C-11, and H-7/C-11, together with the downfield chemical shifts of C-11 ($\delta_C$ 76.8) and C-12 ($\delta_C$ 70.6), assigned a dihydroxy-isopropyl group at C-8. Consequently, the gross structure of **3** was established. The NOESY correlations (Fig. 3) of $CH_3$-15/H-8/$H_2$-12 and $CH_3$-13/H-7 indicated that H-8, $H_2$-12, and $H_3$-15 were $\beta$-oriented, and $H_3$-13 and H-7 were $\alpha$-oriented. By comparison of the experimental and calculated ECD spectra (Fig. 4D), the absolute configuration of **3** was assigned as 1*R*,7*S*,8*R*,11*R*. Thus, the structure of **3** was established and named arpenicarotane A (Fig. S21–S28, supporting information).

Compound **4** was deduced to possess the molecular formula of $C_{15}H_{22}O_4$ by analysis of its HR-ESI–MS data at m/z 265.1439 $[M-H]^-$ (calcd for $C_{15}H_{21}O_4^-$ 265.1440), corresponding to five degrees of unsaturation. The HSQC correlations and 1D NMR data (Table S3, supporting information) of **3** showed the presence of one carbonyl [$\delta_C$ 176.4], two double bonds [$\delta_H/\delta_C$ 4.83 (1H, s), 4.73 (1H, s)/111.9, 5.57 (1H, q, $J=2.4$ Hz)/126.1; $\delta_C$ 149.2, 149.1], two quaternary carbons [$\delta_C$ 79.3, 44.4], two methyls [$\delta_H/\delta_C$ 1.83 (3H, s)/22.3, 1.06 (3H, s)/20.9], two methines [$\delta_H/\delta_C$ 2.79 (1H, d, $J=12.7$ Hz)/51.2, 3.72 (1H, dd, $J=11.6$, 5.2 Hz)], and four methylenes [$\delta_H/\delta_C$ 2.31 (1H, m), 1.29 (1H, m)/22.5; 2.23(1H, m), 1.76 (1H, m)/33.8; 2.08 (1H, dd, $J=13.0$, 5.2 Hz), 1.98 (t, $J=13.0$ Hz)/47.4; 2.15 (1H, d, $J=16.0$ Hz), 2.04 (1H, dd, $J=16.0$, 2.4 Hz)/49.4] (Fig. 2). In the key HMBC correlations (Fig. 3) of $H_3$-15/C-1, C-6, C-7, C-8; of $H_2$-6/C-1, C-4, C-5; of H-5/C-4, C-14; of $H_2$-3/C-1, C-4, C-5, C-14; of $H_2$-2/C-1, C-4, C-7; of H-9/ C-1, C-7, C-8, C-10; and of $H_2$-8/C-15, C-9, combined with the $^1H$-$^1H$ COSY correlations of H-5/$H_2$-6, H-10/H-1, H-1/$H_2$-2 and $H_2$-2/$H_2$-3, a bicyclic system consisted of a cyclopentane fused with a cycloheptane with a methyl located at C-15 and a carboxyl assigned at C-4 could be deduced. Considering the downfield chemical shifts of C-4 ($\delta_C$ 79.3) and C-5 ($\delta_C$ 77.5), two hydroxy groups at C-4 and C-5 could be inferred. Further, HMBC correlations of $H_2$-13/C-12, C-11 and of $H_3$-13/C-10, C-11 established an isopropenyl positioned at C-10. Thus, the planar structure of **4** was established. The NOESY (Fig. 3) correlations of H-13/H-2 and $CH_3$-12/H-9 indicated the *trans*-form for the double bonds $\Delta^{9(10)}$ and $\Delta^{11(13)}$. The NOESY correlations of $CH_3$-15/H-5/H-6 ($\delta_H$ 1.98) and H-1/H-6 ($\delta_H$ 2.08) indicated that $CH_3$-15 and H-5 were $\beta$-oriented, while H-1 and HO-5 were $\alpha$-oriented. The relative configuration of C-4 could not be determined due to a lack of available NOESY correlations. Finally, comparison of the experimental and calculated ECD spectra (Fig. 4E and F) assigned the absolute configuration of **4** as 1*R*,4*R*,5*S*,7*R*. Thus, the structure of **4** was determined and named arpenicarotane B (Fig. S29–S37, supporting information).

The molecular formula of compound **5** was deduced to be $C_{11}H_{10}O_6$ with nine degrees of unsaturation, based on the analysis of its HR-ESI–MS data at m/z 237.0400 $[M-H]^-$ (calcd for $C_{11}H_9O_6$237.0405). The $^1H$ NMR data (Table S4, supporting information) showed a 3H 1,3,5-trisubstituted benzene system at $\delta_H$ 7.19 (1H, t, $J=1.8$ Hz), 7.08 (1H, t, $J=1.8$ Hz), and 6.28 (1H, t, $J=2.3$ Hz), two geminal olefinic protons at $\delta_H$ 5.81 (1H, d, $J=1.68$ Hz) and 5.10 (1H, d, $J=1.68$ Hz), and a methoxy group at $\delta_H$ 3.87 (3H, s). The $^{13}C$ NMR data (Table S4, supporting information) showed the existence of eleven carbon signals, including two carbonyls, eight $sp^2$ carbons, and one methoxy carbon, which were unambiguously designated by the HSQC experiment (Fig. 2). HMBC correlations (Fig. 3) of H-6/C-2, C-4, C-5, C-7; of H-4/C-3, C-5, C-6; of H-2/C-3, C-4, C-7; and of $H_3$-8/C-7 confirmed the presence of 1,3,5-trisubstituted aromatic ring with one hydroxyl and one methoxycarbonyl group positioned at C-5 and C-1, respectively. Further, the key HMBC correlations of $H_2$-11/C-9 and C-10, as well as the downfield chemical shifts of C-3 ($\delta_C$ 158.8), were indicative of a monosubstituted acrylic acid moiety connected to C-3 of the benzene ring through an ether bond. Thus, compound **5** was identified as a new chorismite derivate and named arpenichorismite A (Fig. S38–S44, supporting information).

The remaining known compounds were identified as asperric acid (**6**) (Xing et al. 2019), aspergerthinacid A (**7**) (Pan et al. 2021), 8-O-4-coupled dehydrodiferulic acid (**8**) (Ralph et al. 1994), methy 4-hydroxyphenylacetate (**9**) (Shen et al. 2013), 4-hydroxyphenylacetic acid (**10**) (Ohtani et al. 2011), p-tolyl-3-aminopropanoate (**11**) (Xie et al. 2008), and *p*-(acetylamino) benzoic acid (**12**) (Lewis et al. 2003) by comparison of their NMR spectral data and optical rotation values with those reported in the literature (Fig. S45–S64, supporting information).

## Bioinformatic analysis of the BGCs *Pb_bis* and *Pb_car*

Further detailed investigation of the structures of the metabolites (**1**–**4**) isolated from the co-culture, two different classes of sesquiterpenoids including bisabolene- and carotane-type were characterized. To obtain the encoding gene clusters that potentially might be involved in the biosynthesis of arpenibisabolanes and arpenicarotanes, we examine the genome sequences of *P. brasilianum* and the basidiomycete *A. mellea* (https://mycocosm.jgi.doe.gov/Armme1_1/Armme1_1.home.html) (Li et al. 2023b). Interestingly, three sesquiterpenoids including compounds **2**, **4**, and **6** were also isolated from the genetically modified mutant derived from the strain *P. brasilianum*, in which a pathway-specific activator BerA involving berkeleyacetals biosynthesis from *Neosartorya glabra* was overexpressed (personal communication). This implied that the *P. brasilianum* possessed the capability to biosynthesize the bisabolene- and carotane-type sesquiterpenoids. The biosynthetic locus of aspterric acid has been previously characterized in *Aspergillus terreus* NIH2624; thus, we searched for genomic locus coding enzymes resembling to those encoded by *ast* cluster. The cluster *Pb_car* was ascertained and it is highly homologous to *ast* cluster in the strain *A. terreus* and both clusters exhibited syntenic and highly conserved (Fig. 5A, Table S5, supporting information). Bioinformatic analysis of the cluster *Pb_car* allowed the discovery of genes coding typical enzymes (Fig. 5B), which include the scaffold-forming terpene cyclase (CarA), two post-modification cytochrome P450s (CarB and CarC), and one dihydroxyacid dehydratase (CarD) responsible for self-tolerance.

Arpenibisabolanes (**1**–**2**) are sesquiterpene-derived and the scaffold should be biosynthesized by the sesquiterpene synthase (STS). Therefore, all STSs encoded from two fungal strains were recovered, in which eighteen STSs from *A. mellea* and two hypothetical sesquiterpene synthases from the strain *P. brasilianum* were included. A phylogenetic dendrogram of STSs obtained according to bioinformatic mining from co-culture and previously characterized $\alpha$-bisabolol synthases was constructed, exhibiting a clear separation of terpene synthases (Fig. 5A). In this phylogenetic tree, one synthase designated *Pb*_BisA formed a distinct branch with UbiA-type $\alpha$-bisabolol synthases (BibS) from *Fusarium* sp. JNU-XJ070152 and *Stachybotrys* sp. PYH05-7 (Luo et al. 2022), $\beta$-trans bergamotene synthase from *Aspergillus fumigatus* Af293 (Lin et al. 2013) and plant-derived alpha-bisabolol synthases exemplified as SspiBS from *Santalum spicatum* (Jones et al. 2011), or homologues from *Arabidopsis thaliana* and *Artemisia annua* (Muangphrom et al. 2016; Ro et al. 2006). This indicates it might support the proposal of *Pb*_BisA as a crucial synthase in arpenibisabolanes biosynthesis. DNA sequence analysis of the clustered ~ 7.5 kb *Pb_bis* locus (Fig. 5B), and further amino acid alignment revealed that *Pb*_BisA partakes of 36% identity to alpha-bisabolol synthases from *Stachybotrys* sp. PYH05-7, followed by BibS from *Fusarium* sp. JNU-XJ070152-01 (31% identity) and bergamotene synthase from *A. fumigatus* Af293 (24% identity). In addition to *Pb*-BisA, neighboring genes encoded the cytochrome P450 (BisB), G-protein coupled receptors (GPCR)–like protein (BisC), and decarboxylase (BisD) were also identified. To characterize that the target *Pb*_BisA is responsible for the production of arpenibisabolanes, the *Pb_bisA* was heterologously expressed in yeast *Saccharomyces cerevisiae* BJ5464. Then, a combination of GC–MS analysis with National Institute of Standards and Technology (NIST) Standard Reference Database (v20, 2023–01, https://webbook.nist.gov/) searching revealed that the compound $\beta$-bisabolene (m/z = 204, $C_{15}H_{24}$) could be detected and identified (Fig. S65, supporting information). This reinforced that the target gene cluster *Pb_bis* involved in arpenibisabolanes biosynthesis.

## Hypothetic biogenesis pathway of induced sesquiterpenes

For compounds **1** and **2**, nevertheless, only a few studies have been carried out for scrutinizing the metabolic process of such skeletal unique molecules. Luo et al. characterized the $\alpha$-bisabolol synthases FmaTC and StaTC1 from *Fusarium* sp. and *Stachybotrys* sp., respectively (Luo et al. 2022). These UbiA-type terpene cyclases could produce diverse bisabolene-derived molecules and the pioneering biogenesis insights of bisabolol derivatives were only preliminary. Although compounds **1** and **2** displayed different structures, their primary skeletons are bisabolene-derived. To explain the possible biogenetic origin, their plausible metabolic pathways were proposed in Scheme 1A. Arpenibisabolanes (**1**–**2**) initiate from farnesyl pyrophosphate (FPP) and the enzymatic cyclization generates the intermediate $\beta$-bisabolene. Nevertheless, considering the isolated **1** and **2** that exhibit a wealth of oxygenated modifications, we preferred that a multi-step oxidative cascade occurs after the bisabolene formation step. These conversions might involve one cytochrome P450 monooxygenase (BisB)–catalyzed oxidations. The BisB exhibits a relatively higher identity to the cytochrome P450 (Af510), which catalyzed a cascade of oxidations during fumagillin generation from *Aspergillus fumigatus* (Lin et al. 2013). This implies that BisB might be multifunctional and it was believed to play a key role in generating highly oxygenated structure during arpenibisabolanes biosynthesis. In this scheme, the generation of compound **1** might be modified by auxiliary oxygenases encoded by *Armillaria* species.

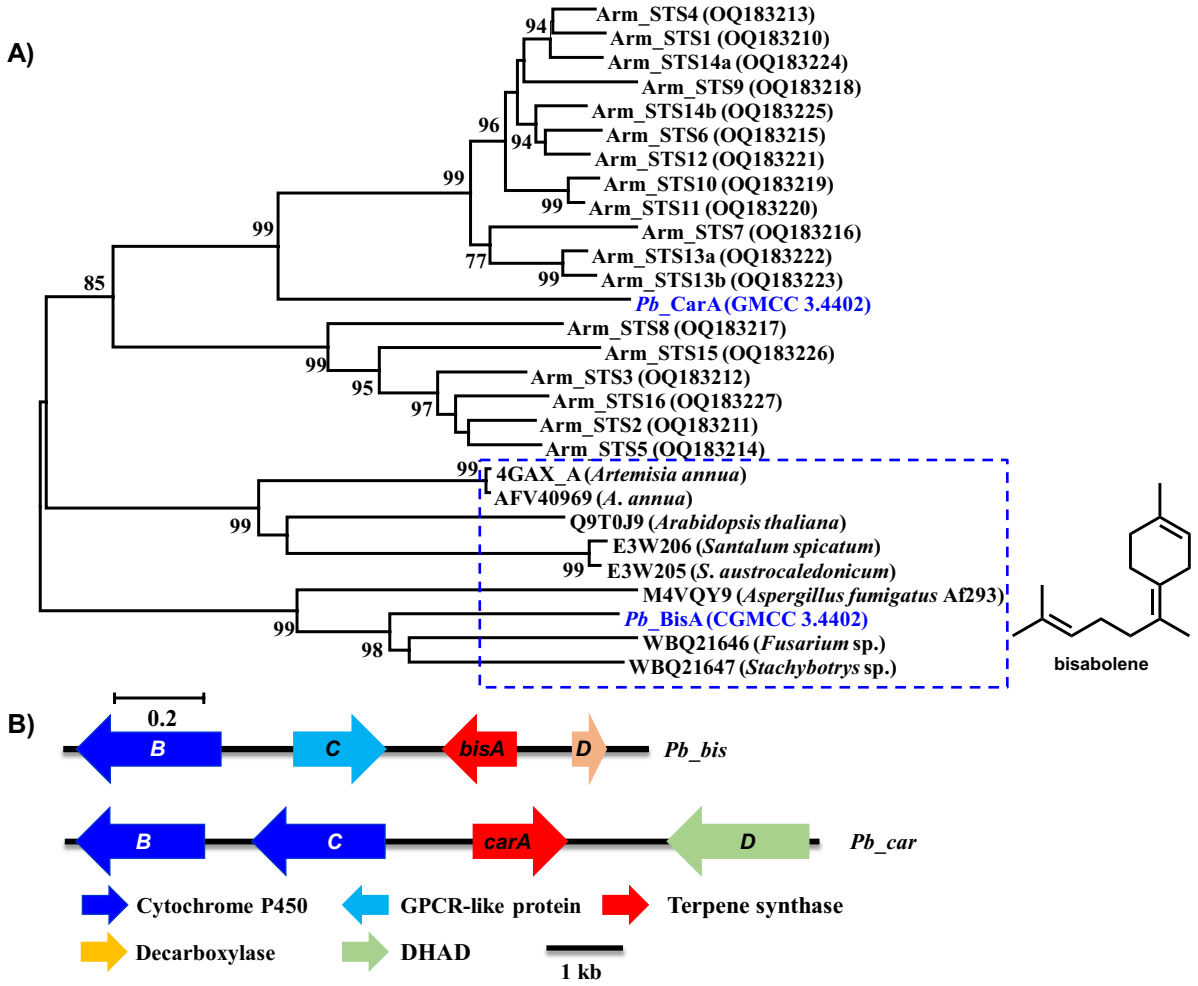


**Fig. 5** Bioinformatic analysis of biosynthetic clusters involved in formation of arpenibisabolanes and arpenicarotanes. **A** Phylogenetic tree of STSs from *P. brasilianum*, *A. mella*, and closely characterized $\alpha$-bisabolol synthases using the Neighbor-Joining method. The scale shows changes per site; numbers at branches are bootstrap values. *Pb*-CarA and *Pb*-BisA are STSs from *P. brasilianum*, Arm_STS1-Arm_STS14b are STSs from *A. mellea*. **B** Putative biosynthetic clusters of isolated metabolites. *Pb_bis* is the encoded cluster of arpenibisabolanes, *Pb_car* is the encoded cluster of arpenicarotanes

Biogenetically, compounds **3**, **4**, and **6** possess a unique carotane-type "5 + 7" bicycle skeleton. Tang and coworkers reconstituted the biosynthesis of aspterric acid and demonstrated that sesquiterpene cyclase AstA and two cytochrome P450s (AstB and AstC) jointly catalyzed the production of aspterric acid (Yan et al. 2018). Thus, as outlined in Scheme 1B, the starter compound FPP was converted into carotane-type key intermediate (-)-daucane catalyzed by terpene cyclase *Pb*_CarA. The intermediate is converted into structurally determined $\alpha$-epoxy carboxylate intermediate iii through CarB-catalyzed multi-step oxidation, in which the epoxy ring might be cleaved to afford trans-1,2-diol intermediate iv. The existence of the intermediate ii is supported by the isolation and characterization of **4** from the strain *P. brasilianum*. The intermediate iv might undergo $C_{15}$-hydroxylation to generate intermediate v, which might be catalyzed by cytochrome P450 CarC. The intermediate iii would then be transformed into the final product aspterric acid, in which the $C_9$–$C_{15}$ $\beta$-ether oxygen moiety was formed. In addition, the biosynthesizing pathway of compound **3** might undergo dihydroxylation of the $C_{11}$–$C_{12}$ ethylene bond. The step of oxidative modification might be catalyzed by a separated oxygenase in *Penicllium* or co-culture pairing strain *Armillaria*.

## Cytotoxic activities of induced representative metabolites

These compounds (**1**–**6**) were evaluated for their cytotoxic activities against MCF-7, A549, and HepG2 cell lines in vitro with cisplatin as the positive control. All six compounds have no obvious inhibition activities against three cell lines (Table S6, supporting information).

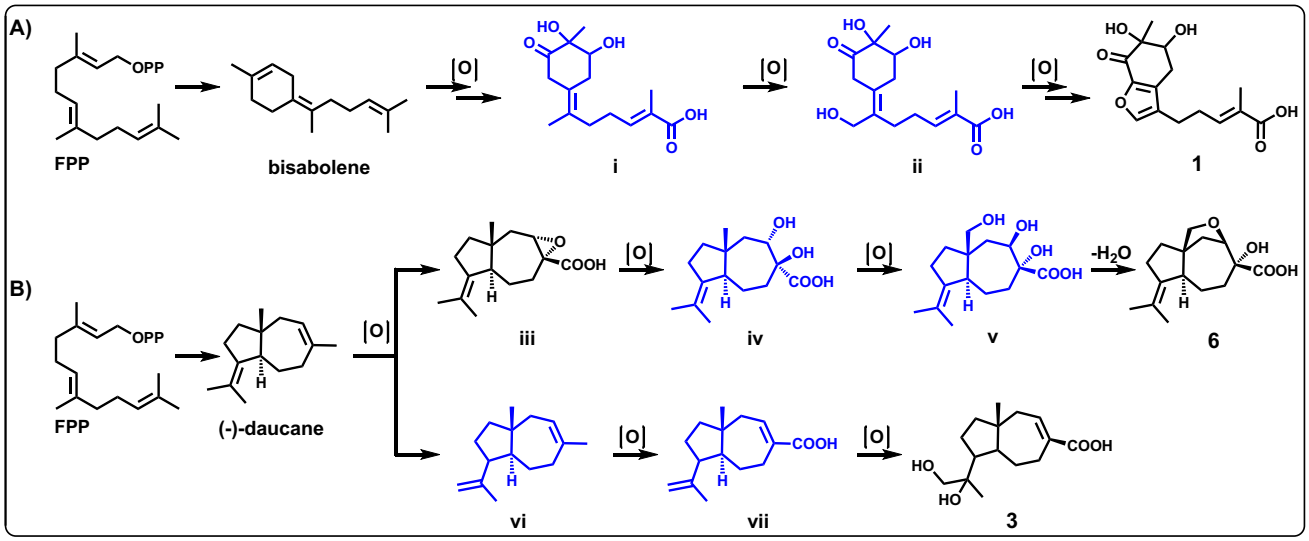


**Scheme 1** Proposed metabolic pathway of arpenibisabolanes and arpenicarotanes biosynthesis

## Discussion

In this report, we have documented the endeavor to unearth the chemical repertoire of co-culture system including *P. brasilianum* and *A. mellea* species. Interestingly, this has led to the discovery of new compounds that were not detected in monoculture. Since the study of the fungal-fungal co-cultivation of *Acremonium* sp. Tbp-5 and *Mycogone rosea* DSM 12973 two decades ago (Degenkolb et al. 2002), the co-culture approach has accelerated the application in mining SMs from fungal species, and numerous compounds exhibiting unique architectures or potent bioactivities have been identified (Goers et al. 2014; Knowles et al. 2022). In addition, with genome sequences becoming accessible due to decreasing costs, genome-guided strategies are now accessible and have revolutionized the discovery of bioactive metabolites (Zhang et al. 2023b, 2022b). Previous studies demonstrated that the transcriptional induction of BGCs is controlled by environmental or interspecies motivation (Knowles et al. 2022; Zhang et al. 2022a). Therefore, considering the biosynthetic potential of the fungus *P. brasilianum*, an OSMAC and a co-culture approach were performed to activate the production of novel SMs, respectively. However, the OSMAC strategy did not exhibit the capability of the strain *P. brasilianum* model (Fig. S1, supporting information). In contrast, during co-culturing with *Armillaria*, the metabolic spectrum of the strain *P. brasilianum* has been markedly broadened and new sesquiterpene compounds were generated (Figs. 1 and 2). Interestingly, previous studies conducted by Ding and colleagues utilized a liquid co-culture system of *Armillaria* sp. and *Epicoccum* sp., and new protoilludane-derived epicoterpenes and armilliphatics A synthesized by *Armillaria* were isolated (Li et al. 2020). But based on our study, nevertheless, the paring fungus *Armillaria* mainly acted as an inducer and most metabolites accumulated in the co-culture were produced by the fungus *P. brasilianum*. This result also highlighted the complexity of the metabolomic process of fungal interspecies interactions, suggesting the different response mechanisms of fungal chemical defenses or inductions (Knowles et al. 2022). Taken together, our present study demonstrates that this approach is a promising strategy to broaden the metabolic patterns of even for well-studied *Penicillium* strains.

To the best of our knowledge, this is the first study that two different categories of sesquiterpenes were identified from the strain *P. brasilianum*. Previous studies have already manifested the metabolic potential of *P. brasilianum* species, and a diverse assortment of bioactive metabolites have been isolated (Bazioli et al. 2017). A more detailed investigation of *P. brasilianum* species and metabolites produced has already been conducted, including the isolate *P. brasilianum* LaBioMMI 024 (producing preaustinoids, verruculogens), the isolate JV-379 (producing brasiliamides), *P. brasilianum* Batista and *Penicillium* sp. MG-11 (producing austin, penicillic acid), *P. brasilianum* NBRC 6234 (producing paraherquonin), the isolate LaBioMMi 136 (producing cyclodepsipeptides JBIR 113), and the isolate FKI-3368 (producing spirohexaline, viridicatumtoxin), for detailed information reference review paper by Bazioli et al. (2017). However, for the strain *P. brasilianum*, no sesquiterpenoids have been reported so far. In our report, conspicuously, the arpenibisabolanes (**1**–**2**) and arpenicarotanes (**3**–**4**) were identified. Arpenibisabolanes **1** and **2** were biosynthesized by bisabolene synthase *Pb*_BisA, which exhibited higher identity to UbiA-type $\alpha$-bisabolol synthase (BibS) from *Fusarium* sp., *Stachybotrys* sp., and *A. absinthium* (Luo et al. 2022;

Muangphrom et al. 2016). Noteworthy, *Pb*_BisA from *P. brasilianum* was distributed in the BibS branch (Fig. 5A). This group of sesquiterpene synthases constitutes a new subfamily and only few fungal-derived BibSs have been characterized (Luo et al. 2022). For the metabolites of carotane-type sesquiterpenes, aspterric acid was first discovered from *A. terreus* IFO-6123 (Tsuda et al. 1978) and the biosynthetic pathway was deciphered using yeast-based heterologous expression platform by Tang and colleagues (Yan et al. 2018). Interestingly, uncommon compounds **1** and **3** exhibited complexified oxidations, e.g., furan ring formation in **1**, and $C_{11}$–$C_{12}$ dihydroxylations in **3**; these biosynthetic processes might be catalyzed by oxygenases from paring *Armillaria* species. New metabolites induced by co-culture including *P. brasilianum* and *A. mellea* revealed a complex molecular mechanism involving interspecies induction or biotransformation.

In the course of our studies, we could not detect the cytotoxic activities of isolated sesquiterpenoids on carcinogenic cell lines. Nevertheless, compound **6** was reported as potent herbicidal agent (Tsuda et al. 1978; Yan et al. 2018). In addition, for the metabolites of bisabolene sesquiterpene derivatives, (*Z*)-12-acetoxybisabol-1-one and 12-acetoxybisabolen-1-ol from *Trichoderma asperellum* EN-764 exhibiting inhibitory activities (4–16 μg/mL) against aquatic pathogens including *Vibrio alginolyticus* and *V. harveyi* were reported (Li et al. 2023a). This implies that the two classes of sesquiterpenoids might function as herbicides or possess antibacterial activities. With the strain and genomic information, our understanding of the biosynthesis of intriguing sesquiterpenoids could be promoted by employing heterologous reconstitution or metabolic engineering strategies.

To summarize, the co-cultivation system of *P. brasilianum* and *A. mellea* was conducted to induce new SMs production and compound discovery. Four novel sesquiterpenoids (**1**–**4**) and one new polyketide **5** were identified from their co-cultivation. Among these, compound **1** possessed a 6/5-fused bicyclic ring scaffold, representing the first example of a 6/5-fused bicyclic bisabolene. These findings will enrich the chemical diversity of sesquiterpenoids and stimulate the interest from academic researchers. Consequently, this study might serve as an example that co-culturing is an attractive approach for broadening the chemical profile of microbes.

**Supplementary Information** The online version contains supplementary material available at https://doi.org/10.1007/s00253-024-13282-4.

**Author contribution** T.Z., L.X.Z., and L.Y. conceived the study. T.Z. obtained initial funding and supervised experiments. T.Z. and X.R. carried out experiments and bioinformatic analysis. L.H.Z. and W.H. elucidated the structures of the compounds. Z.G., J.B., and H.L. conducted the carcinoma cell assay. T.Z. and L.H.Z. wrote the draft manuscript. T.Z. edited the draft manuscript. All authors reviewed the final version of the manuscript.

**Funding** This work was financially supported by the National Natural Science Foundation of China (No. 31872617), the CAMS Innovation Fund for Medical Sciences (CIFMS) (2021-I2M-1–055, 2019-I2M-1–005), the Central Level, Scientific Research Institutes for Basic R & D Fund Business (3332018097), and National Microbial Resource Center, (No. NMRC-2024-3).

**Data availability** The raw read sequences of the biosynthetic gene clusters (*Pb_car* and *Pb_bis*) genes in this study are publicly available in the NCBI database (PP700700 and PP700701). The authors declare that the data supporting the findings of this study are available within the paper and its Supplementary Information files. Should any raw data files be needed in another format, they are available from the corresponding author upon reasonable request.

## Declarations

**Conflict of interest** The authors declare no competing interests.



## References

Ariantari NP, Daletos G, Mandi A, Kurtan T, Muller WEG, Lin W, Ancheeva E, Proksch P (2019) Expanding the chemical diversity of an endophytic fungus *Bulgaria inquinans*, an ascomycete associated with mistletoe, through an OSMAC approach. RSC Adv 9(43):25119–25132. https://doi.org/10.1039/c9ra03678d

Bateman A, Martin MJ, Orchard S, Magrane M, Ahmad S, Alpi E, Bowler-Barnett EH, Britto R, Cukura A, Denny P, Dogan T, Ebenezer T, Fan J, Garmiri P, Gonzales LJD, Hatton-Ellis E, Hussein A, Ignatchenko A, Insana G, Ishtiaq R, Joshi V, Jyothi D, Kandasaamy S, Lock A, Luciani A, Lugaric M, Luo J, Lussi Y, MacDougall A, Madeira F, Mahmoudy M, Mishra A, Moulang K, Nightingale A, Pundir S, Qi GY, Raj S, Raposo P, Rice DL, Saidi R, Santos R, Speretta E, Stephenson J, Totoo P, Turner E, Tyagi N, Vasudev P, Warner K, Watkins X, Zellner H, Bridge AJ, Aimo L, Argoud-Puy GL, Auchincloss AH, Axelsen KB, Bansal P, Baratin D, Neto TMB, Blatter MC, Bolleman JT, Boutet E, Breuza L, Gil BC, Casals-Casas C, Echioukh KC, Coudert E, Cuche B, de Castro E, Estreicher A, Famiglietti ML, Feuermann M, Gasteiger E, Gaudet P, Gehant S, Gerritsen V, Gos A, Gruaz N, Hulo C, Hyka-Nouspikel N, Jungo F, Kerhornou A, Le Mercier P, Lieberherr D, Masson P, Morgat A, Muthukrishnan V, Paesano S, Pedruzzi I, Pilbout S, Pourcel L, Poux S, Pozzato M, Pruess M, Redaschi N, Rivoire C, Sigrist CJA, Sonesson K, Arighi CN, Armin-ski L, Chen CM, Chen YX, Huang HZ, Laiho K, McGarvey P, Natale DA, Ross K,

Vinayaka CR, Wang QH, Wang YQ, Zhang J, Bye-A-Jee H, Zaru R, Sundaram S, Wu CH, Consortium U (2023) UniProt: the universal protein knowledgebase in 2023. Nucleic Acids Res 51(D1):D523–D531. https://doi.org/10.1093/nar/gkac1052

Baumgartner K, Coetzee MP, Hoffmeister D (2011) Secrets of the subterranean pathosystem of *Armillaria*. Mol Plant Pathol 12(6):515–534. https://doi.org/10.1111/j.1364-3703.2010.00693.x

Bazioli JM, Amaral LDS, Fill TP, Rodrigues-Filho E (2017) Insights into *Penicillium brasilianum* secondary metabolism and its biotechnological potential. Molecules 22(6):858. https://doi.org/10.3390/molecules22060858

Bertrand S, Bohni N, Schnee S, Schumpp O, Gindro K, Wolfender JL (2014) Metabolite induction via microorganism co-culture: a potential way to enhance chemical diversity for drug discovery. Biotechnol Adv 32(6):1180–1204. https://doi.org/10.1016/j.biotechadv.2014.03.001

Bills GF, Gloer JB (2016) Biologically active secondary metabolites from the fungi. Microbiol Spectr 4(6):10–128. https://doi.org/10.1128/microbiolspec.FUNK-0009-2016

Blin K, Pascal Andreu V, de Los Santos ELC, Del Carratore F, Lee SY, Medema MH, Weber T (2019) The antiSMASH database version 2: a comprehensive resource on secondary metabolite biosynthetic gene clusters. Nucleic Acids Res 47(D1):D625–D630. https://doi.org/10.1093/nar/gky1060

Bode HB, Bethe B, Höfs R, Zeeck A (2002) Big effects from small changes: possible ways to explore nature's chemical diversity. ChemBioChem 3(7):619–627. https://doi.org/10.1002/1439-7633(20020703)3:7%3c619::AID-CBIC619%3e3.0.CO;2-9

Bouws H, Wattenberg A, Zorn H (2008) Fungal secretomes–nature's toolbox for white biotechnology. Appl Microbiol Biotechnol 80(3):381–388. https://doi.org/10.1007/s00253-008-1572-5

Brase S, Encinas A, Keck J, Nising CF (2009) Chemistry and biology of mycotoxins and related fungal metabolites. Chem Rev 109(9):3903–3990. https://doi.org/10.1021/cr050001f

Cichewicz RH (2010) Epigenome manipulation as a pathway to new natural product scaffolds and their congeners. Nat Prod Rep 27(1):11–22. https://doi.org/10.1039/b920860g

Degenkolb T, Heinze S, Schlegel B, Strobel G, Grafe U (2002) Formation of new lipoaminopeptides, acremostatins A, B, and C, by co-cultivation of *Acremonium* sp. Tbp-5 and *Mycogone rosea* DSM 12973. Biosci Biotechnol Biochem 66(4):883–886. https://doi.org/10.1271/bbb.66.883

Elhamouly NA, Hewedy OA, Zaitoon A, Miraples A, Elshorbagy OT, Hussien S, El-Tahan A, Peng D (2022) The hidden power of secondary metabolites in plant-fungi interactions and sustainable phytoremediation. Front Plant Sci 13:1044896. https://doi.org/10.3389/fpls.2022.1044896

Fradj N, de Montigny N, Merindol N, Awwad F, Boumghar Y, Germain H, Desgagne-Penix I (2020) A first insight into north American plant pathogenic fungi *Armillaria sinapina* transcriptome. Biology (Basel) 9(7):153. https://doi.org/10.3390/biology9070153

Ghoul M, Mitri S (2016) The ecology and evolution of microbial competition. Trends Microbiol 24(10):833–845. https://doi.org/10.1016/j.tim.2016.06.011

Goers L, Freemont P, Polizzi KM (2014) Co-culture systems and technologies: taking synthetic biology to the next level. J R Soc Interface 11(96):20140065. https://doi.org/10.1098/rsif.2014.0065

Jones CG, Moniodis J, Zulak KG, Scaffidi A, Plummer JA, Ghisalberti EL, Barbour EL, Bohlmann J (2011) Sandalwood fragrance biosynthesis involves sesquiterpene synthases of both the terpene synthase (TPS)-a and TPS-b subfamilies, including santalene synthases. J Biol Chem 286(20):17445–17454. https://doi.org/10.1074/jbc.M111.231787

Keller NP (2019) Fungal secondary metabolism: regulation, function and drug discovery. Nat Rev Microbiol 17(3):167–180. https://doi.org/10.1038/s41579-018-0121-1

Kim JH, Lee N, Hwang S, Kim W, Lee Y, Cho S, Palsson BO, Cho BK (2021) Discovery of novel secondary metabolites encoded in actinomycete genomes through coculture. J Ind Microbiol Biotechnol 48(3–4):kuaa001. https://doi.org/10.1093/jimb/kuaa001

Knowles SL, Raja HA, Roberts CD, Oberlies NH (2022) Fungal-fungal co-culture: a primer for generating chemical diversity. Nat Prod Rep 39(8):1557–1573. https://doi.org/10.1039/d1np00070e

Kozlovsky AG, Kochkina GA, Zhelifonova VP, Antipova TV, Ivanushkina NE, Ozerskaya SM (2020) Secondary metabolites of the genus *Penicillium* from undisturbed and anthropogenically altered Antarctic habitats. Folia Microbiol (Praha) 65(1):95–102. https://doi.org/10.1007/s12223-019-00708-0

Lewis EA, Adamek TL, Vining LC, White RL (2003) Metabolites of a blocked chloramphenicol producer. J Nat Prod 66(1):62–66. https://doi.org/10.1021/np020306e

Li H, Tang L, Liu T, Yang R, Yang Y, Zhou H, Ding ZT (2020) Protoilludane-type sesquiterpenoids from *Armillaria* sp. by co-culture with the endophytic fungus *Epicoccum* sp. associated with *Gastrodia elata*. Bioorg Chem 95:103503. https://doi.org/10.1016/j.bioorg.2019.103503

Li H, Li X, Ying Z, Li Y, Wang B (2023) Bisabolane sesquiterpene and cyclopentene derivatives from the marine algal-derived endophytic fungus *Trichoderma asperellum* EN-764. Phytochemistry 210:113644. https://doi.org/10.1016/j.phytochem.2023.113644

Li Y, Feng J, Li J, Li X, Wang H, Yu L, Li J, Zhang T (2023) Diversity and functional research of sesquiterpene synthases in fungus *Armillaria mellea* CPCC 400891. Biotic Resources 45(4):355–364. https://doi.org/10.14188/j.ajsh.2023.04.007

Lin HC, Chooi YH, Dhingra S, Xu W, Calvo AM, Tang Y (2013) The fumagillin biosynthetic gene cluster in *Aspergillus fumigatus* encodes a cryptic terpene cyclase involved in the formation of beta-trans-bergamotene. J Am Chem Soc 135(12):4616–4619. https://doi.org/10.1021/ja312503y

Luo R, Liu B, Xie Y, Li Z, Huang W, Yuan J, He G, Chen Y, Pan Q, Liu Y, Tang J, Wu G, Zhang H, Shi Y, Liu Y, Yu C, Wang B, Lu Y, Han C, Cheung D, Yiu S, Peng S, Zhu X, Liu G, Liao X, Li Y, Yang H, Wang J, Lam T, Wang J (2012) SOAPdenovo2: an empirically improved memory-efficient short-read de novo assembler. Gigascience 1(1):18. https://doi.org/10.1186/2047-217X-1-18

Luo P, Lv J, Xie Y, Xiao L, Qin S, Chen G, Luo X, Hu D, Gao H (2022) Discovery and characterization of a novel sub-group of UbiA-type terpene cyclases with a distinct motif I. Org Chem Front 9(11):3057–3060. https://doi.org/10.1039/D2QO00408A

Lyu HN, Zhang J, Zhou S, Liu HW, Zhuang WY, Li SM, Yin WB (2021) Heterologous expression of a single fungal HR-PKS leads to the formation of diverse 2-alkenyl-tetrahydropyrans in model fungi. Org Biomol Chem 19(38):8377–8383. https://doi.org/10.1039/d1ob01501j

Malit JJL, Leung HYC, Qian P (2022) Targeted large-scale genome mining and candidate prioritization for natural product discovery. Mar Drugs 20(6):398. https://doi.org/10.3390/md20060398

Mao X, Xu W, Li D, Yin WB, Chooi YH, Li Y, Tang Y, Hu Y (2015) Epigenetic genome mining of an endophytic fungus leads to the pleiotropic biosynthesis of natural products. Angew Chem Int Ed Engl 54(26):7592–7596. https://doi.org/10.1002/anie.201502452

Medema MH, de Rond T, Moore BS (2021) Mining genomes to illuminate the specialized chemistry of life. Nat Rev Genet 22(9):553–571. https://doi.org/10.1038/s41576-021-00363-7

Muangphrom P, Seki H, Suzuki M, Komori A, Nishiwaki M, Mikawa R, Fukushima EO, Muranaka T (2016) Functional analysis of amorpha-4,11-diene synthase (ADS) homologs from non-artemisinin-producing *Artemisia* species: the discovery of novel koidzumiol and (+)-alpha-bisabolol synthases. Plant Cell Physiol 57(8):1678–1688. https://doi.org/10.1093/pcp/pcw094

Ohtani K, Fujioka S, Kawano T, Shimada A, Kimura Y (2011) Nematicidal activities of 4-hydroxyphenylacetic acid and oidiolactone

D produced by the fungus *Oidiodendron* sp. Z Naturforsch C J Biosci 66(1–2):31–34. https://doi.org/10.1515/znc-2011-1-205
Oikawa H (2020) Heterologous production of fungal natural products: reconstitution of biosynthetic gene clusters in model host *Aspergillus oryzae*. Proc Jpn Acad Ser B Phys Biol Sci 96(9):420–430. https://doi.org/10.2183/pjab.96.031
Pan R, Bai X, Chen J, Zhang H, Wang H (2019) Exploring structural diversity of microbe secondary metabolites using OSMAC strategy: a literature review. Front Microbiol 10:294. https://doi.org/10.3389/fmicb.2019.00294
Pan G, Li Y, Che X, Tian D, Han W, Wang Z, Zhao Y, Ren S, Xu Y, Hao G, Guo M, Xiao N, Kong F (2021) New thio-compounds and monoterpenes with anti-inflammatory activities from the fungus *Aspergillus* sp. CYH26. Front Microbiol 12:668938. https://doi.org/10.3389/fmicb.2021.668938
Park HB, Park JS, Lee SI, Shin B, Oh DC, Kwon HC (2017) Gordonic acid, a polyketide glycoside derived from bacterial coculture of *Streptomyces* and *Gordonia* species. J Nat Prod 80(9):2542–2546. https://doi.org/10.1021/acs.jnatprod.7b00293
Ralph J, Quideau S, Grabber JH, Hatfield RD (1994) Identification and synthesis of new ferulic acid dehydrodimers present in grass cell walls. J Chem Soc, Perkin Trans 1(23):3485–3498. https://doi.org/10.1039/P19940003485
Ro DK, Ehlting J, Keeling CI, Lin R, Mattheus N, Bohlmann J (2006) Microarray expression profiling and functional characterization of AtTPS genes: duplicated *Arabidopsis thaliana* sesquiterpene synthase genes At4g13280 and At4g13300 encode root-specific and wound-inducible (Z)-gamma-bisabolene synthases. Arch Biochem Biophys 448(1–2):104–116. https://doi.org/10.1016/j.abb.2005.09.019
Rong X, Guo Z, He W, Cai G, Gong K, Wang L, Yu L, Zhang T, Gao K (2023a) Secondary metabolites exhibiting antitumor bioactivities from the fungus *Stachybotrys* sp CPCC 401591. Mycosystema 42(7):1611–1621. https://doi.org/10.13346/j.mycosystema.220342
Rong X, He W, Guo Z, Li X, Wang L, Gao K, Yu L, Zhang T (2023b) Isolation and antitumor activity of phenylspirodrimane derivatives from the fungus *Stachybotrys* sp CPCC 401591. Nat Prod Res Dev 35(8):1348–1356. https://doi.org/10.16333/j.1001-6880.2023.8.007
Shen S, Li W, Wang J (2013) A novel and other bioactive secondary metabolites from a marine fungus *Penicillium oxalicum* 0312F1. Nat Prod Res 27(24):2286–2291. https://doi.org/10.1080/14786419.2013.827190
Sugiyama R, Nakatani T, Nishimura S, Takenaka K, Ozaki T, Asamizu S, Onaka H, Kakeya H (2019) Chemical interactions of cryptic actinomycete metabolite 5-alkyl-1,2,3,4-tetrahydroquinolines through aggregate formation. Angew Chem Int Ed Engl 58(38):13486–13491. https://doi.org/10.1002/anie.201905970
Tsuda Y, Kaneda M, Tada A, Nitta K, Yamamoto Y, Iitka Y (1978) Aspterric acid, a new sesquiterpenoid of carotane group, a metabolite from *Aspergillus terreus* IFO-6123 - X-ray crystal and molecular structure of its para-bromobenzoate. J Chem Soc Chem Comm 4:160–161. https://doi.org/10.1039/c39780000160
Visagie CM, Houbraken J, Frisvad JC, Hong SB, Klaassen CH, Perrone G, Seifert KA, Varga J, Yaguchi T, Samson RA (2014) Identification and nomenclature of the genus *Penicillium*. Stud Mycol 78:343–371. https://doi.org/10.1016/j.simyco.2014.09.001
Wang W, Zeng F, Bie Q, Dai C, Chen C, Tong Q, Liu J, Wang J, Zhou Y, Zhu H, Zhang Y (2018) Cytochathiazines A-C: three merocytochalasans with a 2 H-1,4-thiazine functionality from coculture of *Chaetomium globosum* and *Aspergillus flavipes*. Org Lett 20(21):6817–6821. https://doi.org/10.1021/acs.orglett.8b02942
Wang G, Ran H, Fan J, Keller NP, Liu Z, Wu F, Yin WB (2022) Fungal-fungal cocultivation leads to widespread secondary metabolite alteration requiring the partial loss-of-function VeA1 protein. Sci Adv 8(17):eabo6094. https://doi.org/10.1126/sciadv.abo6094
Weiland-Brauer N (2021) Friends or foes-microbial interactions in nature. Biology (Basel) 10(6):496. https://doi.org/10.3390/biology10060496
Xie X, Mei W, Zeng Y, Lin H, Lin H, Zhuang L, Dai H, Hong K (2008) Cytotoxic constituents from marine actinomycete *Streptomyces* sp. 124092. Chemi J Chin Univ 29(11):2183–2186
Xing CP, Xie CL, Xia JM, Liu QM, Lin WX, Ye DZ, Liu GM, Yang XW (2019) Penigrisacids A-D, four new sesquiterpenes from the deep-sea-derived *Penicillium griseofulvum*. Mar Drugs 17(9):507. https://doi.org/10.3390/md17090507
Yan Y, Liu Q, Zang X, Yuan S, Bat-Erdene U, Nguyen C, Gan J, Zhou J, Jacobsen SE, Tang Y (2018) Resistance-gene-directed discovery of a natural-product herbicide with a new mode of action. Nature 559(7714):415–418. https://doi.org/10.1038/s41586-018-0319-4
Zang Y, Gong Y, Gong J, Liu J, Chen C, Gu L, Zhou Y, Wang J, Zhu H, Zhang Y (2020) Fungal polyketides with three distinctive ring skeletons from the fungus *Penicillium canescens* uncovered by OSMAC and molecular networking strategies. J Org Chem 85(7):4973–4980. https://doi.org/10.1021/acs.joc.0c00147
Zhang T, Zhuo Y, Jia XP, Liu JT, Gao H, Song FH, Liu M, Zhang LX (2013) Cloning and characterization of the gene cluster required for beauvericin biosynthesis in *Fusarium proliferatum*. Sci China Life Sci 56(7):628–637. https://doi.org/10.1007/s11427-013-4505-1
Zhang T, Wan J, Zhan Z, Bai J, Liu B, Hu Y (2018) Activation of an unconventional meroterpenoid gene cluster in *Neosartorya glabra* leads to the production of new berkeleyacetals. Acta Pharm Sin B 8(3):478–487. https://doi.org/10.1016/j.apsb.2017.12.005
Zhang T, Cai G, Rong X, Wang Y, Gong K, Liu W, Wang L, Pang X, Yu L (2022) A combination of genome mining with an OSMAC approach facilitates the discovery of and contributions to the biosynthesis of melleolides from the basidiomycete *Armillaria tabescens*. J Agric Food Chem 70(39):12430–12441. https://doi.org/10.1021/acs.jafc.2c04079
Zhang T, Pang X, Zhao J, Guo Z, He W, Cai G, Su J, Cen S, Yu L (2022) Discovery and activation of the cryptic cluster from *Aspergillus* sp. CPCC 400735 for asperphenalenone biosynthesis. ACS Chem Biol 17(6):1524–1533. https://doi.org/10.1021/acschembio.2c00204
Zhang T, Feng J, He W, Rong X, Lv H, Li J, Li X, Wang H, Wang L, Zhang L, Yu L (2023) Genomic and transcriptomic approaches provide a predictive framework for sesquiterpenes biosynthesis in *Desarmillaria tabescens* CPCC 401429. J Fungi (Basel) 9(4):481. https://doi.org/10.3390/jof9040481
Zhang T, Gu G, Liu G, Su J, Zhan Z, Zhao J, Qian J, Cai G, Cen S, Zhang D, Yu L (2023) Late-stage cascade of oxidation reactions during the biosynthesis of oxalicine B in *Penicillium oxalicum*. Acta Pharm Sin B 13(1):256–270. https://doi.org/10.1016/j.apsb.2022.09.008
Zheng J, Li Y, Liu N, Zhang J, Liu S, Tan H (2022) Multi-omics data reveal the effect of sodium butyrate on gene expression and protein modification in *Streptomyces*. Genom Proteom Bioinform 21(6):1149–1162. https://doi.org/10.1016/j.gpb.2022.09.002
Zhuang L, Zhang H (2021) Utilizing cross-species co-cultures for discovery of novel natural products. Curr Opin Biotechnol 69:252–262. https://doi.org/10.1016/j.copbio.2021.01.023